Virus Filtration Membranes Prepared from Nanoporous Block Copolymers with Good Dimensional Stability under High Pressures and Excellent Solvent Resistance

ARTICLE *in* ADVANCED FUNCTIONAL MATERIALS · MAY 2008

Impact Factor: 11.81 · DOI: 10.1002/adfm.200700832

6 AUTHORS, INCLUDING:

Ji Hoon Park
Institut Pasteur International Network
11 PUBLICATIONS **241** CITATIONS
SEE PROFILE

Jinhwan Yoon
Dong-A University
47 PUBLICATIONS **1,673** CITATIONS
SEE PROFILE

Sung Key Jang
Pohang University of Science and Technology
122 PUBLICATIONS **6,939** CITATIONS
SEE PROFILE

ADVANCED FUNCTIONAL MATERIALS

DOI: 10.1002/adfm.200700832

Virus Filtration Membranes Prepared from Nanoporous Block Copolymers with Good Dimensional Stability under High Pressures and Excellent Solvent Resistance**

By *Seung Yun Yang, Jihoon Park, Jinhwan Yoon, Moonhor Ree, Sung Key Jang,* and *Jin Kon Kim**

We introduce a nanoporous membrane suitable for virus filtration with good dimensional stability under high pressures maintaining high selectivity. The membrane consists of a double layer: The upper layer is a nanoporous film with pore size of ~17 nm and a thickness of ~160 nm, which was prepared by polystyrene-*block*-poly(methyl methacrylate) copolymer (PS-*b*-PMMA) where PMMA block was removed by ultraviolet irradiation followed by rinsing with acetic acid. The nanoporous block copolymer film was combined with a conventional micro-filtration membrane to enhance mechanical strength. The membrane employed in this study did not show any damage or crack even at a pressure of 2 bar, while high selectivity was maintained for the filtration of human rhinovirus type 14 which has a diameter of ~30 nm and is a major pathogen of the common cold in humans. Furthermore, due to crosslinked PS matrix during the UV irradiation, the nanoporous membrane showed excellent resistance to all organic solvents. This could be used under harsh filtration conditions such as high temperature and strong acidic (or basic) solution.

1. Introduction

Separation and purification of bio-molecules such as protein and virus are important processes in biotechnology industry.[1,2] Since the existence of a very small amounts of viruses with a size of tens of nanometers causes severe damage to the entire bio-process, the filtration of viruses has to be perfect.[3] Membrane-based techniques employing ultrafiltration membranes and track-etched membranes have been widely used for virus filtration due to cost effectiveness and ease of operation.[4–9] However, the broad size distribution of pores in ultrafiltration membranes and the low density of pores in track-etched membranes limit the practical use of virus filtration.[6,7]

On the other hand, nanoporous membranes prepared by a block copolymer exhibit uniform sizes of pores due to the self-assembly nature.[10–15] Recently, we reported that nanoporous films prepared by the thin film (~80 nm) of the mixture of polystyrene-*block*-poly(methyl methacrylate) copolymer (PS-*b*-PMMA) and PMMA homopolymer, where only PMMA homopolymer was removed by selective rinsing with acetic acid, have been successfully employed for the filtration of the common cold virus with high selectivity at a low pressure of 0.1 bar.[16] However, this nanoporous membrane has some limits to wide use for virus filtration. First, it does not exhibit good dimensional stability at high filtering pressures (say 0.4 bar) since many cracks are observed after the filtration. Once a crack occurs in a membrane, perfect filtration of virus is impossible. A high filtration pressure is necessary to increase flux and effectively filter waterborne viruses. Secondly, the nanoporous membrane did not show strong adhesion between the nanoporous block copolymer film and a conventional microfiltration membrane, because only PMMA homopolymer was removed by a selective solvent. Also, in this situation, the nanoporous membrane matrix is not crosslinked; the membrane is easily washed out by organic solvents such as toluene or acetic acid.

In this study, we introduce a new nanoporous membrane with good dimensional stability at higher filtration pressures, while maintaining high selectivity for the filtration of viruses. To achieve this objective, we designed a unique nanostructure, namely, vertical orientation of cylindrical pores are only

[*] Prof. J. K. Kim, S. Y. Yang
National Creative Research Initiative Center for Block Copolymer Self-Assembly
Department of Environmental Science and Engineering, and Chemical Engineering
Pohang University of Science and Technology
Kyungbuk 790-784 (Korea)
E-mail: jkkim@postech.ac.kr
J. Park, Prof. S. K. Jang
Departments of Life Sciences, Pohang University of Science and Technology
Kyungbuk 790-784 (Korea)
Dr. J. Yoon, Prof. M. Ree
National Research Lab for Polymer Synthesis and Physics
Department of Chemistry
Pohang University of Science and Technology
Kyungbuk 790-784 (Korea)

[**] This work was supported by the National Creative Research Initiative Program by KOSEF. Synchrotron GISAXS measurements at the Pohang Accelerator Laboratory were supported by the Ministry of Science and Technology and the POSCO. Supporting Information is available online from Wiley InterScience or from the authors.

located near the top and the bottom of the block copolymer film. The vertical orientation of cylindrical nanopores near the top and bottom of the film is necessary for the effective filtration of waterborne viruses. But the middle part of the membrane exhibits a mixed orientation of cylindrical nanopores, that is, a combination of the parallel and perpendicular orientations. The mixed orientation of cylindrical nanopores provides much better mechanical strength (and thus dimensional stability) against hydrodynamic pressure compared with a nanoporous membrane whose cylindrical nanopores are only perpendicularly oriented.[17]

We found that this unique nanostructure was obtained for a relatively thick PS-*b*-PMMA film having ~160 nm where PMMA becomes cylindrical microdomains in the matrix of PS. This film was combined with a commercially available microfiltration membrane to enhance the mechanical strength. To generate nanopores, the cylindrical PMMA microdomains were removed by UV irradiation followed by rinsing with acetic acid. Since UV irradiation gives the covalent coupling between the block copolymer film and the supporting membrane, the adhesion between nanoporous block copolymer film and a microfiltration membrane was much improved compared with the previous nanoporous membrane prepared by the removal of only PMMA homopolymer where crosslinking did not occur.[16] It is also noted that the PS matrix becomes crosslinked during UV irradiation; thus the nanoporous membrane becomes excellent resistance to all kinds of solvents. This membrane does not exhibit any damage or crack even after the filtration at high filtration pressures up to 2 bar, while maintaining high selectivity for the separation of human rhinovirus type 14 (HRV 14) which has a diameter of ~30 nm[18,19] and is a major pathogen of the common cold in humans. We consider that this membrane would be widely used for the filtration of viruses under very harsh conditions such as high temperature and acidic (or basic) solution.

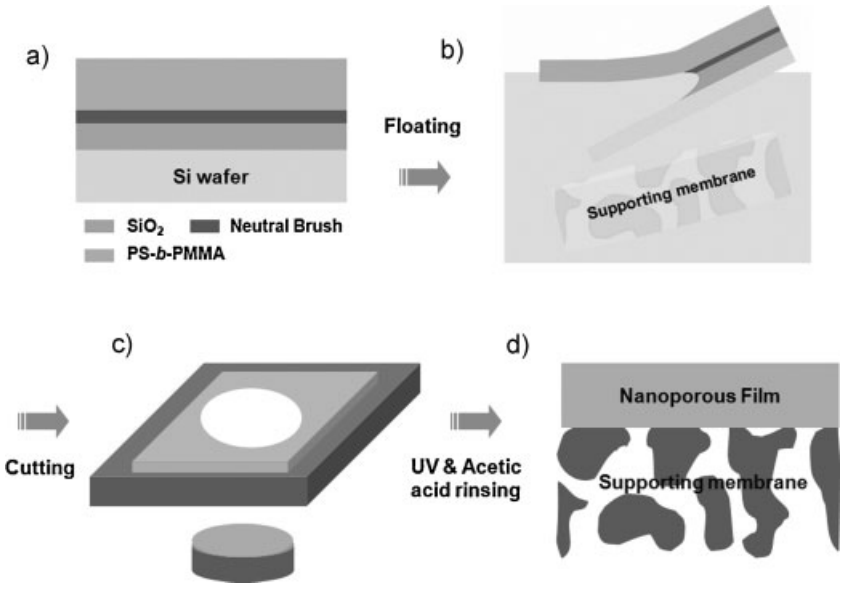

Figure 1. Schematic for the fabrication of asymmetric nanoporous membrane.

2. Results and Discussion

Figure 1 shows a schematic for the fabrication of the nanoporous membranes. The top separation layer was prepared by a film (~160 nm) of PS-*b*-PMMA with cylindrical microdomains of PMMA, on a ~100 nm thick sacrificial silicon oxide layer (Fig. 1a). We found that vertically oriented cylindrical microdomains are observed only near the top and bottom of the block copolymer films, but mixed orientations of cylindrical microdomains are observed inside the film. This film was removed from the silicon substrate by using a buffered hydrofluoric acid (HF) solution to dissolve the oxide layer, and then floated onto a microfiltration polysulfone membrane acting as a supporting material (Fig. 1b). A double layered membrane was properly cut to fit a membrane module (25 mm diameter) (Fig. 1c). Nanoporous thin film in the upper layer was prepared by selectively removing the PMMA block by UV irradiation followed by rinsing with acetic acid (Fig. 1d). This process gives cylindrical nanopores with ~17 nm diameter and very narrow pore size distribution.

Figure 2 shows SEM images for the top, bottom and cross-section of the nanoporous film. The morphology of the bottom side of the film was investigated after flipping over the bottom side to the top of the film, as described in detail in refs. [20,21]. It is seen in Figure 2a that the top surface of film exhibits very narrow size distribution of nanopores with a diameter of ~17 nm. To have effective filtration of the virus, a uniform size distribution of nanopores is essential. Although the packing of pores near the bottom of the film is slightly poorer than that of the top surface, the bottom of the film also exhibits vertically oriented cylindrical nanopores, as shown in Figure 2b. However, the inner film shows quite different morphology compared with the top and bottom parts of the films, as seen in the cross-sectional image (Fig. 2c). Namely, the parallel and perpendicular orientations of cylindrical pores coexist, and it looks like co-continuous nanoporous structure. When a thin film (~80 nm) mixture of the same PS-*b*-PMMA and PMMA homopolymer was used, only perpendicular orientations of cylindrical pores were formed.[16]

To determine in detail the orientation of cylindrical nanopores throughout the entire film, we performed O_2 plasma technique which can etch the film from the surface with an accuracy of nanometer scale.[22] Figure 3 shows SEM images of folded nanoporous films after O_2 plasma etching at various exposure times. The flipped part of the bottom of the film is located on the top surface of the nanoporous film. Before the O_2 plasma etching, vertically oriented cylindrical nanopores were observed in both top and bottom sides of the film (Fig.

ADVANCED FUNCTIONAL MATERIALS

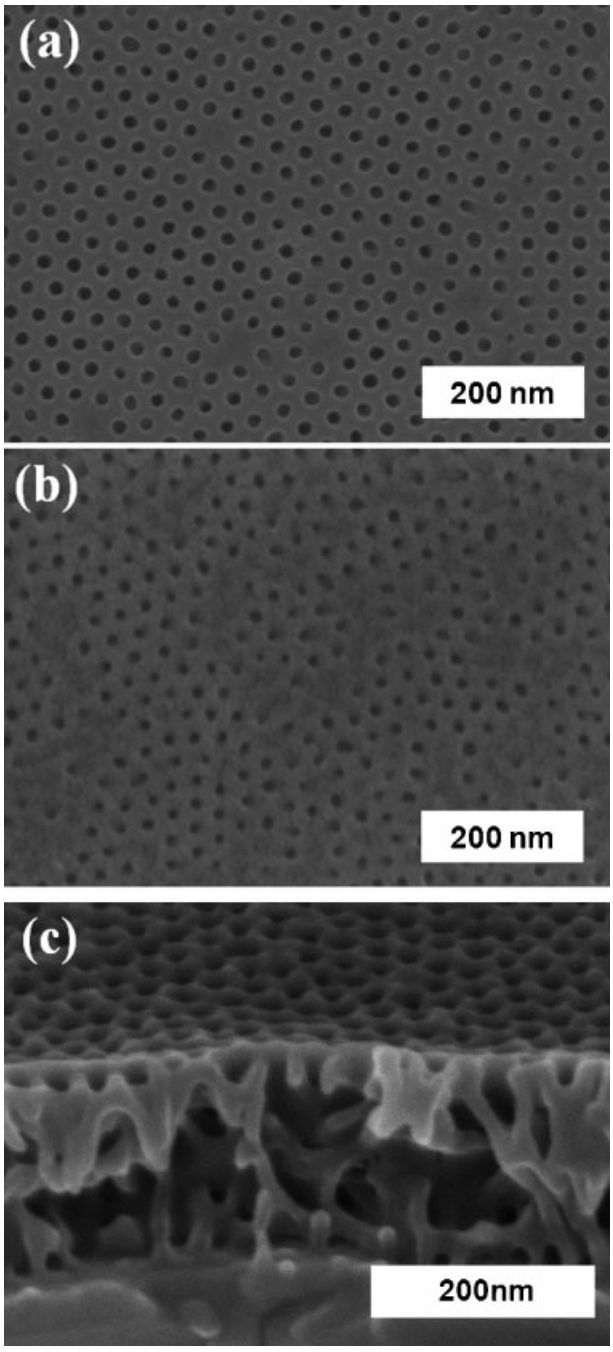

Figure 2. SEM images for the nanoporous film prepared by PS-*b*-PMMA after UV etching followed by rinsing with acetic acid. a) Top surface, b) bottom surface, and c) cross-sectional view. All samples were prepared on a silicon oxide sacrificial layer (~100 nm) and nanoporous film was floated from the sacrificial layer and the bottom surface was flipped over to be placed on the top of the film.

3a). At a 5 s of O_2 plasma etching corresponding to an etched thickness of ~10 nm, the perpendicularly oriented cylindrical nanopores were still maintained for both parts of the film, although the packing of the bottom part looks poorer than that of the top part. However, at 10 s of O_2 plasma treatment, which corresponds to an etched thickness of ~20 nm, parallel

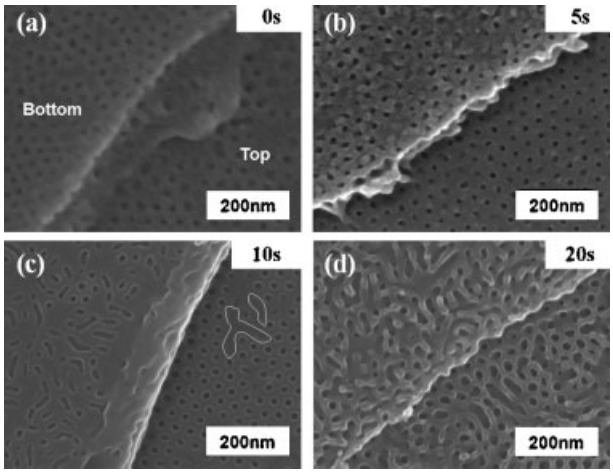

Figure 3. SEM images of the top and bottom parts of the nanoporous film after O_2 plasma etching with different exposure times (s): a) before plasma etching, b) 5, c) 10, and d) 20. The etched rate was determined to be ~2 nm s^{-1}.

oriented cylindrical nanopores (marked by the circles) were for the first time observed at the top surface, and the bottom of the film exhibited mixed orientations of perpendicular and parallel cylindrical nanopores. When the etching time of O_2 plasma was increased to 20 s where the etched thickness is ~40 nm, parallel and perpendicularly oriented nanopores coexist. Therefore, we conclude that the inner part of the film shows mixed orientation of cylindrical nanopores, whereas the top and the bottom surface of the films exhibit perpendicular orientated cylindrical pores. This is consistent with the cross-sectional SEM image given in Figure 2c.

To confirm the mixed orientations of cylindrical nanopores in the film, we carried out grazing incidence small angle X-ray scattering (GISAXS) experiments. Figure 4 shows GISAXS patterns at different incidence angles for the nanoporous film on a silicon substrate. Since the X-ray beam impinges only near the surface region which is the below the critical angle of the film, the details on the depth dependence of the thin-film morphology are easily investigated by controlling the incident angle.[23–26] In this study, a series of incident angles ranging from 0.11 to 0.15° were used to achieve penetration depths from the top surface less than 10 nm to the full penetration in the films (see Fig. S1 in the Supporting Information). At an incidence angle of 0.11°, which corresponds to the X-ray penetration depth of ~9.5 nm from the top surface, high order scattering peaks were clearly detected as shown in Figure 4a, which suggests that cylindrical nanopores are perpendicularly oriented to the substrate.[27] However, a ring pattern was observed at an incidence angle of 0.12°, which corresponds to a penetration depth of ~14.5 nm (Fig. 4b). Also, the GISAXS pattern at an incidence angle of 0.15° corresponding to the full penetration depth shows broad scattering pattern (Fig. 4c). This indicates that the inner film exhibits mixed orientation of cylindrical nanopores. Therefore, we conclude that the nanopores of different types of orientations exist in the nanoporous film: Well-ordered and vertically oriented

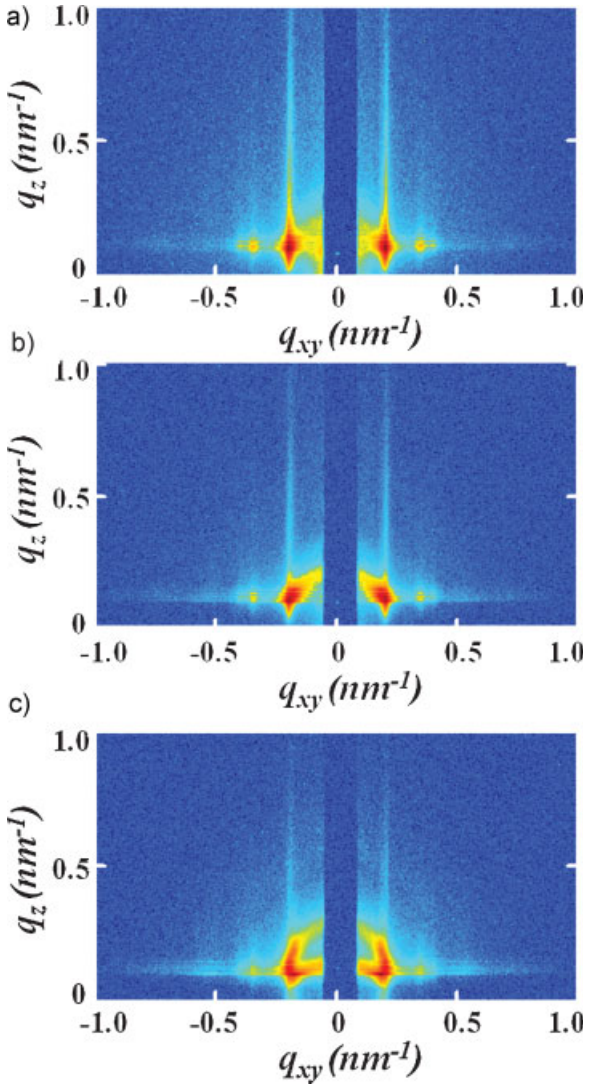

Figure 4. 2D GISAXS patterns at various incidence angles for the nanoporous film on silicon substrate. The incidence angles are a) 0.11°, b) 0.12°, and c) 0.15°.

cylindrical pores are found near the top and bottom part of the film, while mixed oriented cylindrical pores exist in the inner film located ~10 nm below the top surface. This is consistent with results given in Figure 3.

The results shown in Figures 2–4 indicate that the orientation of cylindrical nanopores prepared in this study depends on the film thickness. Cylindrical nanopores located near the top and bottom of the film are vertically oriented, whereas mixed orientations are observed inside the film. Although the detailed mechanism for generating this kind of unique morphology is beyond the scope of this study, we explain this behavior qualitatively as follows. Near the bottom of the film, there exists a neutral brush;[28] thus it is possible to have a perpendicular orientation of PMMA cylindrical nanodomains because of the balanced interaction between each block and the neutral brush. On the other hand, since the PS block with slightly lower surface tension than PMMA block has a slightly better preference to PMMA block near the top (and free) surface, a parallel orientation of PMMA nanodomain is preferred. However, since the length of PS block is larger than PMMA block, the vertical orientation of PMMA nanodomains has some entropy gain compared with the parallel orientation of PMMA nanodomains, as suggested in a theoretical prediction.[29] Thus, perpendicularly oriented PMMA cylindrical nanodomains could be formed near the top surface. We found that the requirement of the volume fraction of PMMA in the PS-*b*-PMMA was strict for having a perpendicular orientation near the top surface. For instance, when the volume fraction of PMMA of another PS-*b*-PMMA was increased to 0.32, most PMMA cylindrical nanodomains show parallel orientation at the top of the film with a thickness of ~160 nm, even though some exhibit perpendicular orientation. The details of the mechanism of perpendicular orientation depending on the volume fraction of PMMA block will be reported in a future publication. Finally, inside the film, the driving force to induce perpendicularly oriented PMMA cylindrical nanodomains from both top and bottom surfaces becomes weak, so that parallel oriented pores coexist with perpendicularly oriented pores.

Figure 5a shows the flux of deionized (DI) water with time through the membrane at various filtering pressures. The pressure was step-wise increased from 0.1 to 0.5 and to 2 bar, and decreased step-wise to the initial value. The flux of DI water increased proportionally to applied pressure, as expected. This means that the membrane was not mechanically damaged at high pressure up to 2 bar. Namely, no crack was observed after the filtration experiment, as demonstrated in Figure 5b.

The increased mechanical stability is due to the unique morphology of the nanoporous film having mixed morphology inside the film, even though the film was crosslinked and twice thicker than another nanoporous film with perpendicular pore structure employed in ref. [16]. The film thickness could enhance the mechanical stability of the film. However, we found that the maximum pressure for a nanoporous membrane with perpendicular pore structure to be mechanically stable was ~0.3 bar, which is ~1/6 of that for the film with mixed pore morphology. It is noted that when the pressure was increased to 0.4 bar, many cracks were observed for this nanoporous film (see Fig. S2 in the Supporting Information).

To investigate crosslinking effect on the mechanical stability of the film, we carried out permeation experiment for DI water by using a crosslinked nanoporous membrane with perpendicular orientation with a thickness of ~80 nm. We found that many cracks were observed at the film surface after the filtration even at 0.2 bar (see Fig. S3 in the Supporting Information). On the other hand, another nanoporous membrane with a thickness of ~80 nm, which was prepared by selective rinsing of PMMA homopolymer,[16] no crack was observed. Therefore, we consider that the crosslinking process of PS matrix did not increase the mechanical stability of the film. Rather, since it makes the nanoporous film brittle, the mechanical stability might be worse. Thus, we consider that the

ADVANCED FUNCTIONAL MATERIALS

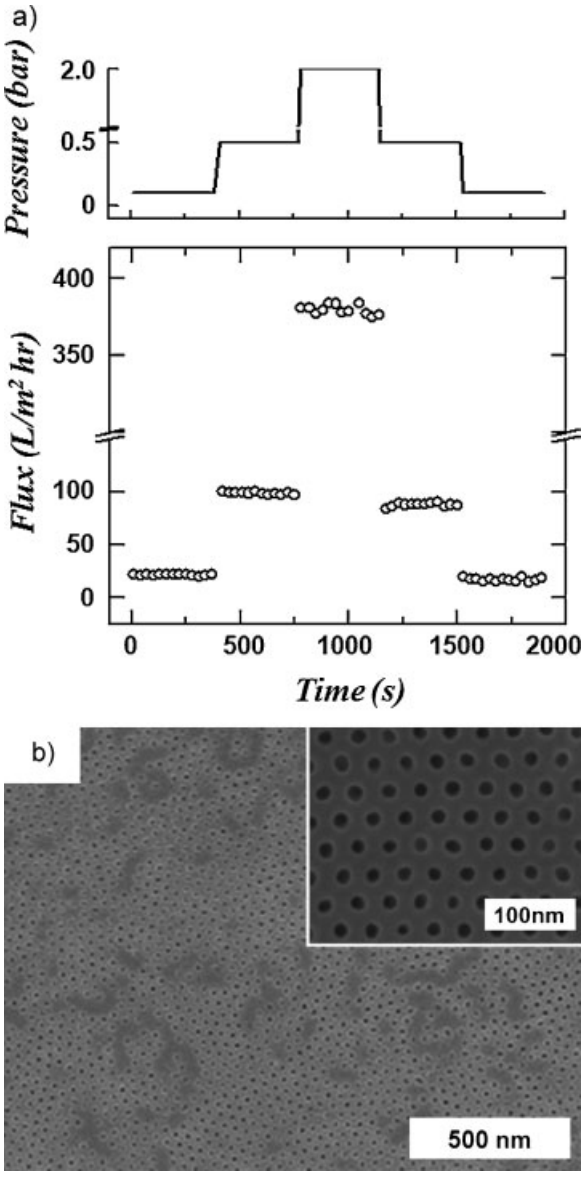

Figure 5. a) Flux of DI water with time at three different pressures (0.1, 0.5 and 2 bar) for the nanoporous membrane employed in this study. b) SEM image for the surface of the nanoporous membrane after the permeability experiment, showing no mechanical damage (or crack) in the membrane.

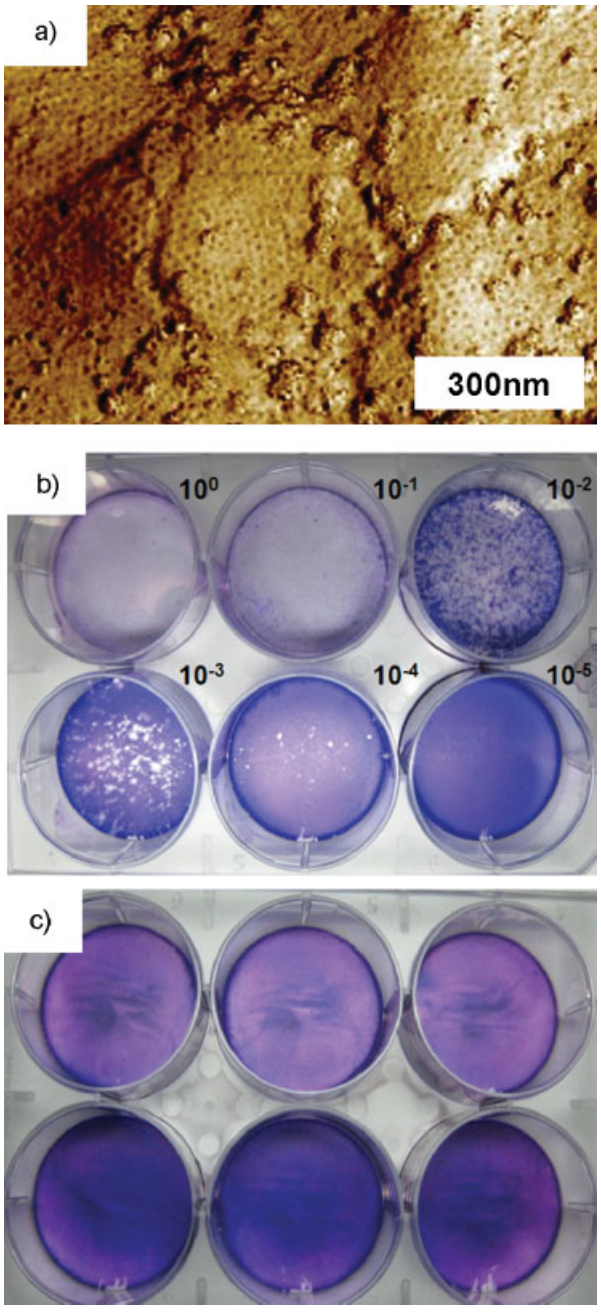

Figure 6. a) AFM phase image of the top of the nanoporous membrane after filtration of PBS solution containing 4×10^6 PFU ml^{-1} of HRV 14. Plaque assays of HRV 14 solution before (b) and after (c) the filtration through the nanoporous membrane. Serially diluted solutions were applied to the monolayers of HeLa cells. The well at the upper left corner contains virus from 0.2 ml of original solution penetrated through a filter, and each well is consecutively diluted by a factor of 10 up to the dilution of 10^5 for the well at the lower right corner.

pore structure is a major factor to determine the mechanical stability of the film.

Figure 6 shows atomic force microscope (AFM) images of the top of the nanoporous membrane after the filtration of crude virus solution (5 ml) containing HRV 14 virions and the results of plaque assay of HRV 14. A filtration experiment was carried out at a constant pressure of 0.5 bar and stirring speed of 200 rpm. Although a pre-filtration was performed by using 0.1 μm pore-sized filter (MillexVV, Millipore), the large sized biomaterials in crude virus solution could not be completely removed by the filter. Thus, the surface of the nanoporous membrane was covered by various types of the cell debris. The exact structure of the virus can be obtained from the purified virus solution, as shown in our previous report.[16] Here, we used a crude virus solution to evaluate the possibility of practical uses such as haemodialysis. Although the surface of nanoporous membrane was covered by various types of biomolecules which might reduce the flux at a given pressure, any mechanical damage such as crack was not observed in this

membrane after the filtration. The most important experiment for virus solution is the plaque assay, and the results before and after the filtration are shown in Figure 6b and c, respectively. The concentration (4×10^6 PFU ml^{-1}) of virus solution before the filtration was calculated from the number of plaques (white circles). We found that no plaque was observed from the filtered solutions, indicating that the nanoporous membrane employed in this study completely blocks all virus particles in the solution from penetration through the membrane. Although we could not increase the filtration pressure up to 2 bar due to the limited amount of HRV 14 virions, the perfect filtration for HRV virions could be anticipated at this pressure because the crack was not observed at the film after the filtration of DI water at 2 bar (see Fig. 5).

Finally, we investigate the stability of the nanoporous membrane against various organic solvents and acidic (or basic) solution. Since the nanoporous separation layer was prepared by removing cylindrical PMMA block by UV irradiation process, the PS matrix was crosslinked.[30,31] This indicates that the membrane studied in this study exhibits excellent resistance to all kinds of solvent. Figure 7 shows the SEM images of the top surface of nanoporous thin film after it was immersed into various solvents for 6 h at a high temperature (for instance, near the boiling points of all solvents). Regardless of solvents, well-ordered cylindrical pores are clearly maintained. Thus, we consider that the nanoporous membrane could be used for the perfect filtrations of the viruses existing in the organic and acidic (or basic) solutions when solvent-resistant membranes made of polytetrafluoroethylene or polyvinylidene fluoride (for instance, Zefluor or FP Vericel^{TM}, Pall Co.) are used as the supporting membrane.

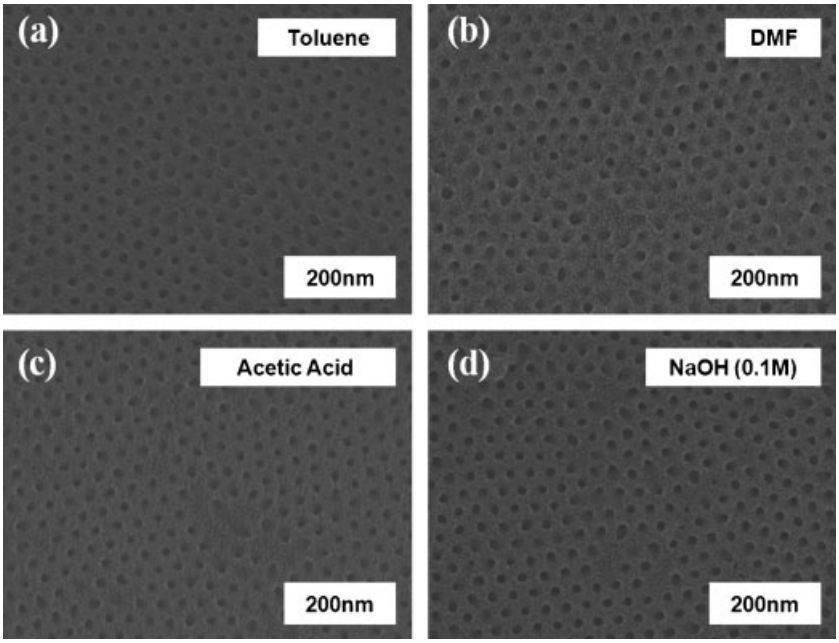

Figure 7. SEM images of the top surface in the nanoporous block copolymer film after soaking into various solvents for 6 h at 70 °C: a) toluene; b) dimethyl formamide; c) acetic acid (glacial grade); d) 0.1 M of aqueous NaOH.

3. Conclusions

A double layered nanoporous membrane suitable for virus filtration with good dimensional stability under high pressures and excellent solvent resistance, while maintaining the high selectivity, was introduced. The upper layer, as used for the separation of the viruses, is a nanoporous film with a pore size of ~17 nm and a thickness of ~160 nm, which was prepared by the PS-*b*-PMMA film. The cylindrical nanopores are perpendicularly oriented near the top and bottom of the film, whereas inside the film mixed orientations of parallel and perpendicular cylindrical nanopores are observed. The mixed oriented cylindrical nanopores allow much higher mechanical strength under high pressures compared to a membrane with only perpendicularly oriented cylindrical nanopores. Namely, this membrane prepared in this study did not show any damage or crack even at a pressure of 2 bar, while maintaining high selectivity for the filtration of human rhinovirus type 14. Furthermore, due to crosslinked PS matrix during the UV irradiation, the nanoporous membrane showed excellent resistance to all of organic solvents. This could be used under harsh filtration conditions such as high temperature and strong acidic (or basic) solution.

4. Experimental

An asymmetric polystyrene-*block*-poly(methyl methacrylate) copolymer (PS-*b*-PMMA) with an average molecular weight of 77,000 g mol^{-1} and polydispersity of 1.06 was prepared by anionic polymerization. The volume fraction of PMMA block was 0.25. A hydroxy end-functionalized random copolymer of styrene and methyl methacrylate, denoted PS-*r*-PMMA, having a styrene fraction of 0.6, was synthesized in bulk *via* a TEMPO "living" free radical polymerization. The molecular weight was 9,600 g mol^{-1} with polydispersity of 1.80 [28]. PS-*r*-PMMA was spin coated on a silicon oxide sacrificial layer with a thickness of 100 nm which was evaporated onto a silicon wafer and then annealed at 170 °C under vacuum for two days. This procedure allowed the coupling reaction between hydroxyl group of PS-*r*-PMMA and oxygen group available in the silicon oxide layer. A thin layer (~6 nm) of PS-*r*-PMMA remained on the surface after rinsing with toluene.

A relatively thick film (~160 nm) of the PS-*b*-PMMA was prepared by spin coating of 4% (w/v) toluene solutions onto the modified silicon wafers and then annealed at 170 °C under vacuum for two days, and quenched to room temperature. The PMMA cylindrical microdomains were etched out by UV irradiation using a UV lamp (model G15T8, Sankyo Denki, Japan) with the highest intensity at 253.7 nm for 3 hr under a vacuum and then immersed in acetic acid for 1 h at room temperature. The nanoporous films were dried in vacuum for 12 h at room temperature.

For the O_2 plasma etching, the specimen was placed in a vacuum chamber (Plasma Prep II, Spi) maintaining O_2 pressure of 100 mTorr and 10 W RF power. Under this etching condition, the film was etched at a rate of ~2 nm s^{-1}. The morphology of the films was examined by using field emission scanning electron microscopy (FESEM, Hitachi S-4800) operating at 3 kV.

ADVANCED FUNCTIONAL MATERIALS

GISAXS measurements were carried out at the 4C2 beamlines of the Pohang Accelerator Laboratory [24,25]. The sample-to-detector distance was 2125 mm; an X-ray radiation source of $\lambda = 0.1336$ nm and a two-dimensional charge-coupled detector (2D CCD: Roper Scientific, Trenton, NJ, USA) were used. Samples were mounted on a 4-circle goniometer (Huber, Rimsting, Germany) equipped with a vacuum chamber. The incidence angle of the X-ray beam was changed from 0.11 to 0.15° to investigate the film morphology depending on the penetration depth of the X-ray beam. Scattering angles were corrected by the positions of X-ray beams reflected from the silicon substrate interface with changing incidence angle and by precalibrated polystyrene-*block*-polyethylene-*block*-polybutadiene-*block*-polystyrene copolymer. A set of aluminum foil strips were employed as semi-transparent beam stops because the intensity of the specular reflection from the substrate is much stronger than the intensity of GISAXS near the critical angle. GISAXS patterns were collected for 10 s.

To make the nanoporous membrane, phase-separated block copolymer films were floated onto the surface of a 5 wt% HF solution and then transferred to a porous membrane supports with a diameter of 47 mm (HT Tuffryn™, Pall Life Science). The supporting membrane had an average pore diameter of 0.2 μm and a thickness of 150 μm [16]. This double-layered membrane was cut to 25 mm disc by using a punch and then pores were prepared by UV irradiation followed by rinsing with acetic acid.

Permeation experiments were performed at a stirring speed of 200 rpm at room temperature in a stirred cell module (Amicon 8010, Millipore). The stirred cell has a 10 ml working volume and an effective membrane area of 4.1 cm^2. This module was connected by a reservoir with a volume of 800 ml (Amicon 800, Millipore). The nanoporous membrane was immersed in ethanol for 1 h to enhance the wetting of the aqueous solution to the nanopores prior to loading into preautoclaved stirred cell. Excess ethanol was completely removed by flushing with deionized water for at least 30 min. The morphology of deposited virions on the membranes was investigated by Atomic force microscopy (AFM, Digital Instrument D3000) with silicon nitride tips on cantilevers (Nanoprobe) in the tapping mode.

Cultivation and purification of HRV14 was performed as described by Erickson et al. [18]. A virus solution (5 ml) [4×10^6 PFU ml^{-1} in phosphate buffered saline (PBS)] was forced to pass through filters, and then plaque assays [32] were performed by using solutions penetrating through the filters. HeLa/E cells were grown in a 35-mm petri dish with Dulbecco's modified eagles medium, 1% penicillin/streptomycin and 10% fetal bovine serum. The HeLa cells were washed once with PBS and once with a serum-free medium. The solutions penetrated through the filters were serially diluted (10 fold) and then applied to the cells. The first well in each dish contains viruses from 0.2 ml of the permeated solutions. An overlaid medium, composed of Dulbecco's modified eagles medium, 1% penicillin/streptomycin, 5% fetal bovine serum and 50% gum tragacanth, was added to the virus-infected cells and then incubated for 3 days. After the virus cultivation, the overlaying medium was removed and then plaques were visualized with 0.5% crystal violet dissolved in 70% ethanol.

Received: July 25, 2007
Revised: November 1, 2007

[1] D. B. Burns, A. L. Zydney, *Biotechnol. Bioeng.* **1999**, *64*, 27.
[2] M. Ulbricht, *Polymer* **2006**, *47*, 2217.
[3] D. M. Bohonak, A. L. Zydney, *J. Membr. Sci.* **2005**, *254*, 71.
[4] P. Roberts, *Rev. Med. Virol.* **1996**, *6*, 25.
[5] S. B. Lee, D. T. Mitchell, L. Trofin, T. K. Nevanen, H. Söderlund, C. R. Martin, *Science* **2002**, *296*, 2198.
[6] S. R. Wickramasinghe, B. Kalbfuß, A. Zimmermann, V. Thom, U. Reichl, *Biotechnol. Bioeng.* **2005**, *92*, 199.
[7] T. Urase, K. Yamamoto, S. Ohgaki, *J. Membr. Sci.* **1996**, *115*, 21.
[8] C. C. Striemer, T. R. Gaborski, J. L. McGrath, P. M. Fauchet, *Nature* **2007**, *445*, 749.
[9] X. B. Ke, H. Y. Zhu, X. P. Gao, J. W. Liu, Z. F. Zheng, *Adv. Mater.* **2007**, *19*, 785.
[10] C. Park, J. Yoon, E. L. Thomas, *Polymer* **2003**, *44*, 6725.
[11] C. J. Hawker, T. P. Russell, *MRS Bull.* **2005**, *30*, 952.
[12] R. A. Segalman, *Mater. Sci. Eng. R* **2005**, *48*, 191.
[13] G. Liu, J. Ding, *Adv. Mater.* **1998**, *10*, 69.
[14] A. S. Zalusky, R. Olayo-Valles, J. H. Wolf, M. A. Hillmyer, *J. Am. Chem. Soc.* **2002**, *124*, 12761.
[15] W. A. Phillip, J. Rzayev, M. A. Hillmyer, E. L. Cussler, *J. Membr. Sci.* **2006**, *286*, 144.
[16] S. Y. Yang, I. Ryu, H. Y. Kim, J. K. Kim, S. K. Jang, T. P. Russell, *Adv. Mater.* **2006**, *18*, 709.
[17] W. C. Young, *Roark's Formulas for Stress and Strain*, McGraw-Hill, New York **1989**.
[18] J. W. Erickson, E. A. Frankenberger, M. G. Rossmann, G. S. Fout, K. C. Medappa, R. R. Rueckert, *Proc. Natl. Acad. Sci. USA* **1983**, *80*, 931.
[19] M. G. Rossmann, *Nature* **1985**, *317*, 145.
[20] U. Jeong, H. C. Kim, R. L. Rodriguez, I. Y. Tsai, C. M. Stafford, J. K. Kim, C. J. Hawker, T. P. Russell, *Adv. Mater.* **2002**, *14*, 274.
[21] U. Jeong, D. Y. Ryu, J. K. Kim, D. H. Kim, T. P. Russell, C. J. Hawker, *Adv. Mater.* **2003**, *15*, 1247.
[22] R. Magerle, *Phys. Rev. Lett.* **2000**, *85*, 2749.
[23] M. Tolan, *X-Ray Scattering from Soft-Matter Thin Films*, Springer, New York **1999**.
[24] B. Lee, W. Oh, Y.-T. Hwang, Y.-H. Park, J. Yoon, K. S. Jin, K. Heo, J. Kim, K.-W. Kim, M. Ree, *Adv. Mater.* **2005**, *17*, 696.
[25] B. Lee, Y.-H. Park, Y.-T. Hwang, W. Oh, J. Yoon, M. Ree, *Nat. Mater.* **2005**, *4*, 147.
[26] B. Lee, I. Park, J. Yoon, S. Park, J. Kim, K.-W. Kim, T. Chang, M. Ree, *Macromolecules* **2005**, *38*, 4311.
[27] J. Yoon, S. Y. Yang, B. Lee, W. Joo, K. Heo, J. K. Kim, M. Ree, *J. Appl. Crystallogr.* **2007**, *40*, 305.
[28] P. Mansky, Y. Liu, E. Huang, T. P. Russell, C. Hawker, *Science* **1997**, *275*, 1458.
[29] Q. Wang, P. F. Nealey, J. J. de Pablo, *Macromolecules* **2001**, *34*, 3458.
[30] K. Shin, K. A. Leach, J. T. Goldbach, D. H. Kim, J. Y. Jho, M. Tuominen, C. J. Hawker, T. P. Russell, *Nano Lett.* **2002**, *2*, 933.
[31] U. Jeong, D. Y. Ryu, D. H. Kho, J. K. Kim, J. T. Goldbach, D. H. Kim, T. P. Russell, *Adv. Mater.* **2004**, *16*, 533.
[32] B. Hahm, S. H. Back, T. G. Lee, E. Wimmer, S. K. Jang, *Virology* **1996**, *226*, 318.